Fluid elasticity-enhanced insulator-based dielectrophoresis for sheath-free particle focusing in very dilute polymer solutions

Mahmud Kamal Raihan, Micah Baghdady, Heston Dort, Joseph Bentor, and Xiangchun Xuan*

Department of Mechanical Engineering, Clemson University, Clemson, SC 29634, USA

* Corresponding author. Email: xcxuan@clemson.edu (Dr. Xuan). Fax: 864-656-7299.

ABSTRACT

Focusing particles into a narrow stream is usually a necessary step in microfluidic flow cytometry and particle sorting. We demonstrate the addition of a small amount of polyethylene oxide (PEO) polymer into a buffer solution can reduce by almost one order of magnitude the threshold DC electric field for single-line dielectrophoretic focusing of particles in a constricted microchannel. The particle focusing effectiveness of this fluid elasticity-enhanced insulator-based dielectrophoresis, or E-iDEP short, in very dilute PEO solutions gets enhanced with the increase of the PEO molecular weight and particle size. These two trends are both consistent with a theoretical analysis that accounts for the fluid elasticity effects on the electrokinetic and dielectrophoretic particle motions. Surprisingly, the particle focusing effectiveness of E-iDEP is observed to first increase and then decrease with the increase of the PEO concentration.

INTRODUCTION

Microfluidic devices have been widely used to handle particles (either synthetic or biological) for chemical, biomedical, and environmental applications.[1-5] Focusing particles into a narrow stream is usually a necessary step in many of these devices such as flow cytometer and particle sorter.[6-10] Both externally imposed (e.g., acoustic,[11-13] electric,[14-16] magnetic,[17-19] etc.) and internally induced (e.g., inertial[20-23] and elastic[24-27] lift) forces have been utilized to move particles across streamlines for sheath-free focusing. Among these *active* and *passive* particle focusing methods, insulator-based dielectrophoresis (iDEP)[28-30] has received increasing interest because of its easy and robust operation in electrokinetic microfluidic devices that favor integration and automation for point-of-care technologies. This technique exploits an insulating hurdle on a channel wall or simply the insulating wall itself if with a nonzero curvature to create local electric field gradients for inducing the dielectrophoretic force.[31,32] It has thus far been demonstrated to focus, trap, concentrate and sort particles for various microfluidic applications.[33-35]

One of the simplest iDEP devices for sheath-free particle focusing is a rectangular microchannel with a single widthwise constriction, wherein particles suspended in a more-conductive fluid are directed towards the channel centerline by negative DEP.[36] In such a constricted microchannel, a high-magnitude DC electric field usually must be used in order to achieve a single-line particle focusing unless the size of the particles closely matches that of the constriction.[37] Under this circumstance, Joule heating and other negative effects will probably cause issues to the sample and even the device itself.[38,39] Two primary approaches have been

developed to enhance the iDEP focusing in constricted microchannels: one is to increase the DEP force and the other is to extend the particles' exposure time to the DEP force. For the first approach, adding an AC component to the DC electric field contributes to the DEP force, but does not change the electrokinetic particle motion or the acting time of DEP.[36,40] Alternatively, replacing the one-dimensional widthwise constriction with a two-dimensional one in both the channel width and depth planes leads to a larger channel-to-constriction ratio and hence a stronger DEP force.[41] For the second approach, the use of a linear[42] or a two-dimensional array[43] of constrictions has been demonstrated to enhance the iDEP focusing, where the particle exposure to DEP is elongated at the cost of increasing space. In particular, our recent work proposed the use of AC electric field for iDEP focusing of particles in a virtually "infinite" microchannel.[44] The effectiveness of such AC-iDEP focusing was found to be a quadratic function of the AC field magnitude, distinct from the linear dependence in DC (including DC-biased AC) field driven iDEP devices.[14,15]

Another potential approach to improved iDEP focusing is re-suspending particles into non-Newtonian fluids, whose rheological effects have been demonstrated to strengthen the hydrodynamic flow induced lift force enabling an effective focusing of smaller particles than in Newtonian fluids.[45-48] Our group has recently conducted experiments to investigate the iDEP focusing of particles in several polymer solutions that are all in the semidilute-entangled state. Lu et al.[49] observed an oscillatory motion for particles traveling along with the DC electroosmotic flow of viscoelastic polyethylene oxide (PEO) solutions, which was found to not stop until a sufficient number of particles formed a chain leaving the constriction of the microchannel. Lu et

al.[50] later reported a weaker focusing effect for particles traveling against the electroosmotic flow of PEO solutions than in a PEO-free buffer solution with no sign of particle oscillation. Moreover, this weakened iDEP focusing in the PEO solutions shows a decreasing trend with the increase of DC electric field, opposite to that in a Newtonian fluid. In a more recent paper, Bentor et al.[51] performed an experimental study of the fluid shear-thinning effect on the iDEP focusing of particles in two other types of semidilute polymer solutions through the same constricted microchannel. They observed a significantly improved particle focusing phenomenon in the strongly shear-thinning and viscoelastic polyacrylamide (PAA) solution as compared to the Newtonian buffer under the same DC electric field. In contrast, the particles in the strongly shear-thinning but (nearly) inelastic xanthan gum (XG) solution were found to remain unfocused because of perhaps the strongly disturbed electroosmotic flow in the constriction region.[52]

We report in this work a surprising finding that the use of very dilute PEO solutions, in contrast to the semidilute polymer solutions in previous studies,[49-52] can substantially reduce the DC electric field for iDEP focusing of particles in a constricted microchannel. We examine how the variations of the PEO molecular weight and concentration, respectively, may affect this fluid elasticity-enhanced iDEP (E-iDEP) for sheath-free particle focusing. We also examine the role of particle size in such an E-iDEP focusing. Moreover, we attempt to explain the experimental observations using a theoretical analysis that accounts for the possible fluid elasticity effects on the electrokinetic and dielectrophoretic particle motions.

MATERIALS AND METHODS

Experimental Setup

Figure 1a shows a photo of the constricted microchannel used in the experiment. The mold for the channel was fabricated by photolithography with SU-8 2025 (Kayaku Advanced Materials). The channel was then obtained from the mold using the standard soft lithography technique with polydimethylsiloxane (PDMS). The details about the procedure can be found in our previous paper.[36] The microchannel is 500 μm wide and 1 cm long with a 50 μm wide and 250 μm long constriction in the middle. It has a measured height of 55 μm everywhere. The particle solutions were prepared by re-suspending spherical polystyrene particles (Sigma Aldrich) into 1 mM phosphate buffer-based dilute PEO solutions (Sigma Aldrich). They were each mixed with 0.5% v/v Tween 20 (Fisher Scientific) surfactant to suppress the particle-particle interactions and particle-wall adhesions. The particle concentration was kept low in all the solutions to reduce the particle-particle interactions. The electric conductivity of the prepared PEO solutions was measured to be around 150 μS/cm, which can be safely viewed much larger than that of polystyrene particles.[53]

The reference parameters in our experiment were selected as 10 μm particles in 50 ppm PEO solution with a molecular weight, $M_w = 2$ MDa. For the effect of particle size on iDEP focusing, we tested 5, 10 and 15 μm diameter particles (Sigma Aldrich). For the effect of polymer concentration, we tested $c = 30$, 50, 100, 200, and 400 ppm PEO solutions with $M_w = 2$ MDa. The pure buffer solution, i.e., PEO free or $c = 0$, was also tested as a control test. For the effect

of polymer length, we tested $M_w = 0.3$, 0.6, 1, 2, 4 and 8 MDa PEO solutions at a fixed concentration of 50 ppm. The overlap concentrations for these PEO polymers can be estimated from $c^* = 0.77/\left(0.072{M_w}^{0.65}\right)$,[54] which were found to decrease from 2945 to 348 ppm with the increase of M_w from 0.3 to 8 MDa. Hence, our prepared PEO solutions are all in the dilute regime exhibiting a weak to negligible shear thinning effect.[55] The elasticity effect of the PEO solutions is characterized by the Weissenberg number,[56]

$$Wi = \lambda\dot{\gamma} \tag{1}$$

where λ is the relaxation time and $\dot{\gamma}$ is the fluid shear rate. The value of the effective relaxation time was estimated from,[57] $\lambda = 18\lambda_Z(c/c^*)^{0.65}$, where λ_Z is the Zimm relaxation time given by,[58] $\lambda_Z = F\frac{[\eta]M_w\eta_s}{N_A k_B T}$. In this definition, the pre-factor, $F = 0.463$, was estimated from the Remann Zeta function using a solvent quality exponent of 0.55,[59] $\eta_s = 1.0$ mPa·s is the solvent viscosity, N_A is the Avogadro's constant, k_B is the Boltzmann's constant, and T = 293.15 K is the room temperature. Table 1 presents the estimated rheological properties for each of our prepared PEO solutions.

Table 1. Rheological properties for the prepared fluids. The Weissenberg number was estimated using the electrokinetic particle velocity, U_{EK}, within the constriction of the microchannel under 100 V DC voltage.

Solution	M_w (MDa)	c (ppm)	c^* (ppm)	$\frac{c}{c^*}$	λ_Z (ms)	λ (ms)	U_{EK} (mm/s)	G_{EK}	Wi
Pure buffer	–	–	–	–	–	0	2.9	–	0
PEO	0.3	50	2945	0.017	0.015	0.019	1.1	0.37	0.00081

0.6	50	1877	0.027	0.047	0.080	0.96	0.33	0.0031
1	50	1346	0.037	0.11	0.23	0.93	0.32	0.0086
2	50	858	0.058	0.34	0.97	0.90	0.31	0.035
4	50	457	0.091	1.1	4.1	0.78	0.27	0.13
8	50	348	0.14	3.4	17	0.77	0.27	0.53
2	30	858	0.035	0.34	0.69	1.1	0.39	0.032
2	100	858	0.12	0.34	1.5	0.88	0.30	0.053
2	200	858	0.23	0.34	2.4	0.83	0.29	0.079
2	400	858	0.47	0.34	3.7	0.79	0.27	0.12

The prepared particle solution was driven through the constricted microchannel using DC electric fields generated by a high-voltage DC power supply (Glassman High Voltage, Inc.). The magnitude of the imposed DC electric field never exceeded 400 V/cm in the experiment to avoid the effect of strong Joule heating. Under this electric field, the electric current through the microchannel was observed to increase by no more than 2% within 3 mins, indicating at most a 1 ºC temperature rise if the fluid conductivity is assumed to have a 2% temperature coefficient.[38] The influence of electrothermal flow is therefore considered minimal because of the dominance of electroosmosis under pure DC electric fields.[60] Moreover, the time span for electric field application was kept no more than 1 min to further minimize the influence of Joule heating as well as the pressure-driven backflow. The liquid heights in the two end-channel reservoirs were balanced out prior to every test to prevent the effect of hydrostatic pressure on particle motion. Each test was performed at least three times to confirm the consistency, among which no significant discrepancies were noticed. Particle motion in the constriction region was visualized and recorded using a microscope (Nikon Eclipse TE2000U, Nikon Instruments) equipped with a

CCD camera (Nikon DS-Qi1Mc). The captured digital images were processed using the Nikon imaging software (NIS-Elements AR 2.30).

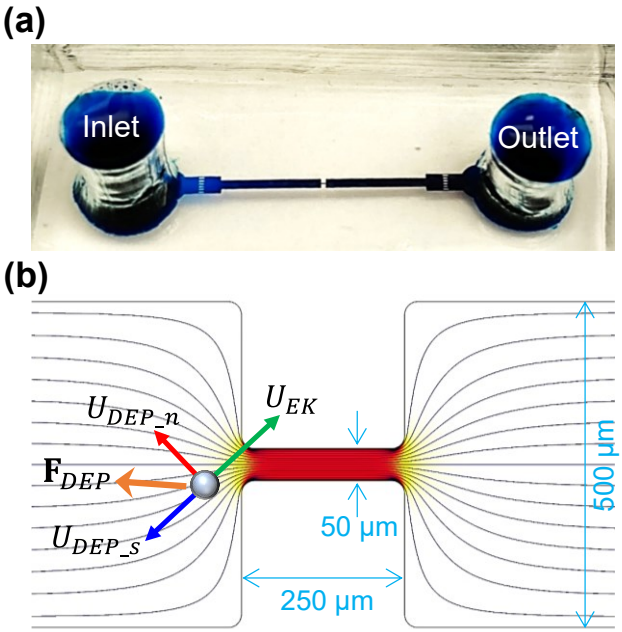

Figure 1. (a) Photo of the microfluidic chip (the constricted microchannel and reservoirs are filled with blue food dye for visualization) used in the experiment; (b) Schematic illustration of iDEP focusing of particles in the constriction region of the microchannel. The electric field gradient (see the contour of $\nabla\mathbf{E}^2$ in the background, the darker color the larger magnitude)-induced dielectrophoretic force, $\mathbf{F}_{DEP}$, generates both a cross-stream (see the electric field lines, which are similar to the streamlines for purely electrokinetic flows of Newtonian fluids[14]) particle motion, U_{DEP_n}, which focuses particles to the centerline of the channel, and a streamwise particle motion, U_{DEP_s}, which opposes the electrokinetic particle motion, U_{EK}, and hence facilitates the particle focusing and trapping.

Theoretical Analysis

The presence of the insulating constriction in the microchannel gives rise to local electric field gradients (see the background contour of electric field squared in Figure 1b), yielding a dielectrophoretic force, $\mathbf{F}_{DEP}$, on the suspended particles,[14]

$$\mathbf{F}_{DEP} = \frac{1}{4}\pi d^3 \varepsilon f_{CM} \nabla \mathbf{E}^2 = -\frac{1}{8}\pi d^3 \left(\frac{\partial \mathbf{E}^2}{\partial s} \hat{\mathbf{s}} + 2\frac{\mathbf{E}^2}{\mathcal{R}} \hat{\mathbf{n}} \right) \quad (2)$$

where d is the particle diameter, ε is the fluid permittivity, f_{CM} is the Clausius-Mossotti factor depending only on the particle and fluid conductivities for DC electric fields,[39] $\mathbf{E}$ is the electric field vector, s denotes the streamline direction with $\hat{\mathbf{s}}$ being its unit vector, $\mathcal{R}$ is the radius of curvature of the streamline, and $\hat{\mathbf{n}}$ is the unit vector normal to the streamline. As they are much less conductive than the suspending fluid, polystyrene particles experience negative DEP in our experiments with $f_{CM} \cong -0.5$ and are thus directed towards the lower electric field region. Note that the two terms for the $\hat{\mathbf{s}}$ and $\hat{\mathbf{n}}$ directions within the bracket of eq 2 are obtained from the analogy to the acceleration components along and normal to the streamline direction, respectively.[36] The dielectrophoretic particle velocity, $\mathbf{U}_{DEP}$, is developed by balancing $\mathbf{F}_{DEP}$ with the Stokes drag, where the latter has been demonstrated to depend on the fluid elasticity and shear thinning,[61]

$$\mathbf{U}_{DEP} = U_{DEP\_s}\hat{\mathbf{s}} + U_{DEP\_n}\hat{\mathbf{n}} = -\frac{\mu_{DEP}}{G_D(Wi)} \left(\frac{\partial \mathbf{E}^2}{\partial s} \hat{\mathbf{s}} + 2\frac{\mathbf{E}^2}{\mathcal{R}} \hat{\mathbf{n}} \right) \quad (3)$$

In the above, U_{DEP_s} and U_{DEP_n} are the components of $\mathbf{U}_{DEP}$ along and normal to the streamline, respectively, and $\mu_{DEP} = d^2\varepsilon/24\eta_0$ is the traditional definition for the dielectrophoretic particle mobility in the Newtonian solvent with η_0 being its viscosity.[14] $G_D(Wi)$ is the correction factor that we introduce here to account for the potential effects of polymer addition to the Newtonian solvent on the Stokes drag, which may include, for example, the fluid elasticity and polymer viscosity etc.[62,63]

The cross-stream dielectrophoretic motion, U_{DEP_n}, causes the particles, which travel through the constriction region of the microchannel at the streamwise electrokinetic velocity, $U_{EK} = G_{EK}(Wi)\mu_{EK}E$, to migrate towards the channel centerline. Such an iDEP focusing effect is governed by the following dimensionless particle velocity ratio,[14]

$$\left|\frac{U_{DEP\_n}}{U_{EK}}\right| = \frac{1}{G_D(Wi)G_{EK}(Wi)}\frac{2\beta E}{\mathcal{R}} \tag{4}$$

$$\beta = \frac{\mu_{DEP}}{\mu_{EK}} = \frac{d^2}{24(\zeta_p - \zeta_w)} \tag{5}$$

In the above, $G_{EK}(Wi)$ is another correction factor we introduce here to account for the potential effects of polymer addition to the Newtonian solvent on the electrokinetic particle velocity,[64,65] $\mu_{EK} = \varepsilon(\zeta_p - \zeta_w)/\eta_0$ is the traditional definition of the electrokinetic particle mobility with ζ_p and ζ_w being the particle and wall zeta potentials in the Newtonian solvent, and β is the dielectrophoretic-to-electrokinetic mobility ratio. The streamwise dielectrophoretic motion, U_{DEP_s}, opposes the electrokinetic motion of particles, and hence facilitates the particle focusing. Moreover, with the increase of the imposed electric field, U_{DEP_s} may become sufficiently large to stagnate the particles at the entrance of the constriction region for a local trapping. The threshold electric field for such an iDEP trapping effect, E_{tr}, is given by,

$$\frac{\partial E_{tr}}{\partial s} = G_D(Wi)G_{EK}(Wi)\frac{1}{2\beta} \tag{6}$$

It is therefore the product of the two introduced correction factors, $G_D(Wi)$ and $G_{EK}(Wi)$, that characterizes the overall impact of polymer addition to the Newtonian solvent (here, represented simply by the fluid elasticity in terms of Wi) on both the iDEP focusing and trapping of particles in PEO solutions. While both correction factors are assumed to be associated with the

polymer addition via the altered fluid viscosity and elasticity etc., they are not necessarily equal because the fluid rheological effects on electroosmotic flow and electrophoretic motion may follow dissimilar trends to those on the Stoke drag. Moreover, the polymer addition can affect other physicochemical properties such as the wall and particle zeta potentials[66] that are pertinent to G_{EK} only. We must admit that the above analysis neglects the influence of nonlinear electrophoresis of particles because the electric conductivity of our suspending buffer solution is much larger than that of the particles and hence the surface conduction effect becomes insignificant.[67,68] Also neglected in our analysis is the influence of nonlinear electroosmosis of fluids (e.g., electrothermal flow and induced-charge electroosmosis)[38] because of the dominating linear electroosmosis under pure DC electric fields.[60,69,70] These two assumptions together lead to a linear electrokinetic particle motion or alternatively an electric field-independent electrokinetic mobility.[71] Our model should be used with appropriate modifications when the fluid conductivity becomes comparable to that of the suspended particles and/or AC (or DC-biased AC) electric fields are employed to drive the particle suspension.

Owing to the dependence of Wi on both the fluid relaxation time and shear rate in eq 1, the effectiveness of iDEP focusing and trapping should be affected by the PEO concentration and molecular weight as well as the electric field magnitude. The value of Wi was estimated from $Wi = 2\lambda U_{EK}/w_c$ using the electrokinetic particle velocity inside the constriction of width w_c, which was obtained by multiplying the measured average velocity for 3-5 particles away from the constriction under 100 V DC voltage with the channel-to-constriction width ratio (i.e., 10 here).

The value of U_{EK} (see Table 1) was found insensitive to the size of the particles used in our tests, consistent with our recent experiment.[68] Moreover, it exhibits only a slightly decreasing trend with the increase of polymer concentration or molecular weight. This is reflected by the observation of $G_{EK}(Wi) = 0.33 \pm 0.06$ (note the error is less than 20%) in Table 1, which was obtained by comparing U_{EK} in each of the prepared PEO solutions with the measured particle velocity in the Newtonian buffer. The calculated Wi exhibits an increasing trend with the increase of PEO concentration or molecular weight in Table 1. It is, however, smaller than 1, indicating a weak elasticity effect in all cases.

RESULTS AND DISCUSSION

Demonstration of E-iDEP

Figure 2a shows the images of 10 μm diameter particles in 50 ppm, 2 MDa PEO solution in the constriction region of the microchannel. The particles, which are nearly evenly scattered before the constriction, exhibit a strong focusing effect downstream towards the center of the channel under the DC voltage as low as 50 V. The corresponding DC electric field over the channel length is 50 V/cm on average while that inside the constriction has a magnitude of 500 V/cm because of the mismatch between the channel and constriction widths. The former value of average electric field will be used below for the discussion, consistent with that typically employed for iDEP devices.[14,15] A single-line focusing of the particles is achieved at around 90 V/cm. Increasing the DC field to 120 V/cm initiates a partial trapping of the particles while a complete trapping takes

place at around 200 V/cm. In contrast, the traditional iDEP focusing of 10 μm particles in the pure buffer solution, which is the Newtonian solvent of the PEO solution, is apparently weaker than in the PEO solution as viewed from the images in Figure 2b. Specifically, the single-line particle focusing in the Newtonian fluid does not occur until the DC electric field reaches 400 V/cm, which is about 4.4 times the value in the PEO solution. We see from Table 1 that the electrokinetic particle velocity in the PEO solution is about 31% of that in the Newtonian buffer, i.e., $G_{EK}(Wi) = 0.31$, which is viewed reasonable considering the polymer addition-induced increase in both fluid viscosity and elasticity[65] as well as the possible changes in other physicochemical properties such as zeta potential.[66] Thus, to explain the difference in the electric field for single-line particle focusing in between the PEO and buffer solutions using eq 4, we need $G_D(Wi) = 0.73$ such that $1/G_D(Wi)G_{EK}(Wi) = 4.4$. This seems reasonable too as $G_D(Wi) < 1$ has been reported to arise from the fluid elasticity-caused drag reduction.[62] We will present in the next three sections a quantitative investigation of the parametric effects on the E-iDEP focusing of particles.

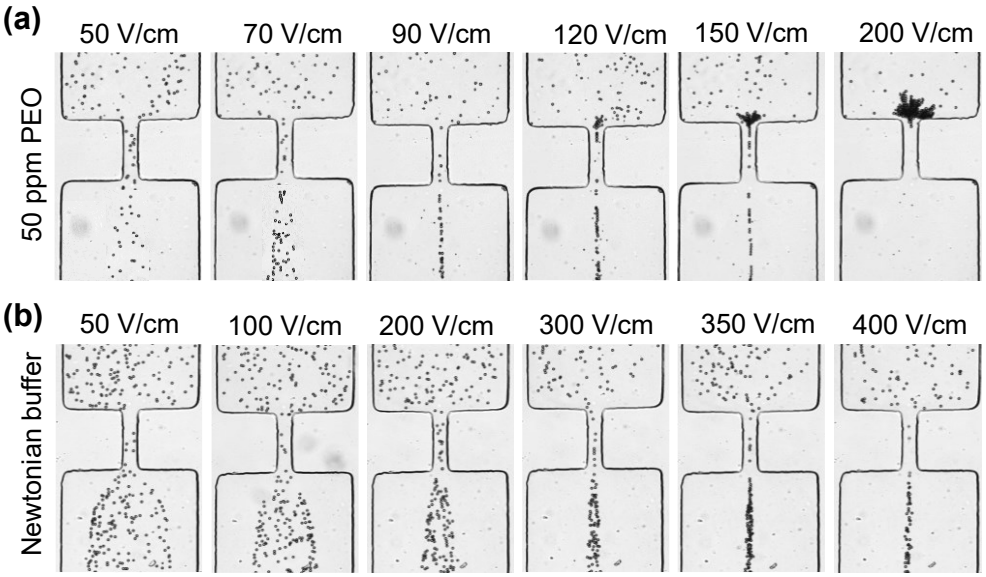

Figure 2. Top-view snapshot images comparing the iDEP focusing of 10 μm diameter particles in the flow of (a) 50 ppm, 2 MDa PEO and (b) Newtonian buffer solutions in the constricted microchannel. The magnitude of the imposed DC electric field (averaged over the channel length) is labeled on top of each image. The particle moving direction is from top to bottom in all images.

Effect of Polymer Molecular Weight

Figure 3 shows the images of 10 μm particles in 50 ppm PEO solutions with different polymer molecular weights, M_w, in the constricted microchannel over a range of DC electric fields. There is an apparently increasing trend in the E-iDEP focusing of particles with the increase of M_w under each electric field. Even in the PEO solution with the smallest $M_w = 0.3$ MDa, the particle focusing drastically gets enhanced against the pure buffer solution in Figure 2b. The particles in this least viscoelastic PEO solution reach a single-line focusing at around 210 V/cm (data not shown in Figure 3) as compared to 400 V/cm in the Newtonian buffer. The increase of M_w further reduces the required electric field for the single-line particle focusing to around 140, 120, 80 and 50 V/cm in the 0.6, 1, 4 and 8 MDa PEO solutions, respectively. The onset of particle trapping

also shifts towards the lower electric field regime in the higher-M_w PEO solutions. Such an improving trend in the E-iDEP focusing and trapping of particles with the increase of M_w may be explained by the decrease of both $G_{EK}(Wi)$ (see Table 1) and $G_D(Wi)$ in eqs. 4 and 6. Interestingly, for the PEO solution with the largest $M_w = 8$ MDa, particles start experiencing disturbances in the constriction region as the electric field reaches above 70 V/cm, leading to an unstable focusing position and even oscillation. This phenomenon seems qualitatively consistent with our recent observation in 100 ppm (and higher), 4 MDa PEO solutions,[49] for which the underlying reason is currently unclear.

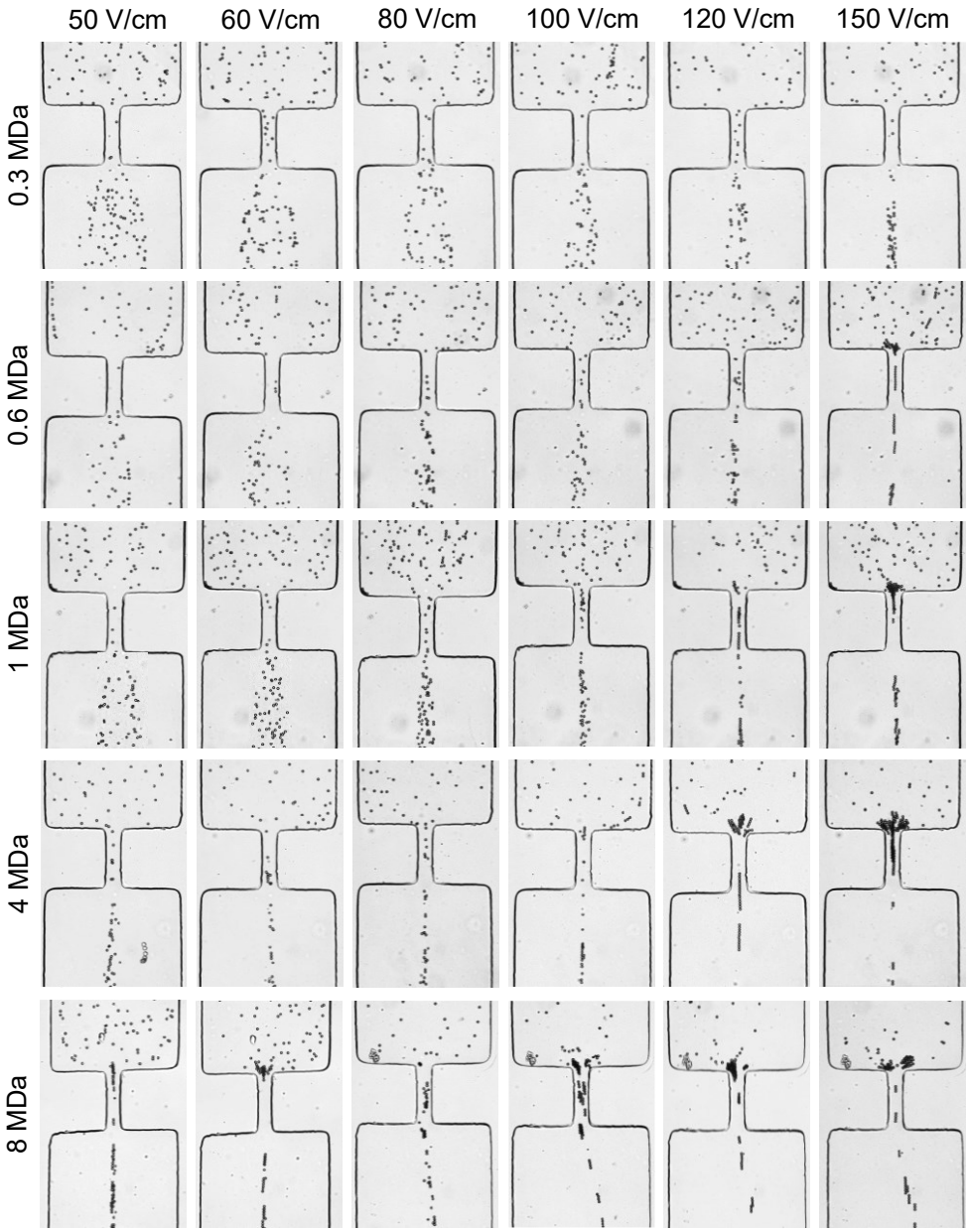

Figure 3. Top-view snapshot images demonstrating the effect of PEO molecular weight (labeled to the left of each row) on the E-iDEP focusing of 10 μm diameter particles in 50 ppm PEO solutions in the constricted microchannel. The magnitude of the imposed DC electric field is labeled at the top of each column. The particle moving direction is from top to bottom in all images.

To evaluate the focusing of particles, we define a dimensionless focusing effectiveness, *FE*,

$$FE = \frac{d}{w_p} \quad (7)$$

where w_p is the width of the particle stream after the constriction that can be measured directly from the superimposed images. A larger *FE* indicates a better focusing of particles, and its maximum value is unity corresponding to a single-line focusing regardless of the particle size. Figure 4a plots the particle *FE* vs. DC electric field in the Newtonian buffer and PEO solutions with different M_w. Two clear trends can be viewed from this figure: one is the increase of *FE* with the increase of PEO molecular weight under each electric field, which is attributed to the decrease of the product of $G_D(Wi)$ and $G_{EK}(Wi)$ in eq 4 as a result of the increasing Wi. This trend is further illustrated in Figure 4b for a fixed electric field of 80 V/cm. The other trend is the increase of *FE* with the increase of electric field as expected from eq 4, for which the experimental data in each fluid can be fitted to a power trendline with a better than 90% R-squared value. Moreover, the power of this electric field dependence achieves a larger value in the higher-M_w PEO solution as seen from Figure 4b though the rate of increase with M_w slows down and eventually levels out. Specifically, it increases from roughly 1 in the Newtonian buffer, which agrees with the linear-dependence prediction of eq 4 for $G_D(Wi)G_{EK}(Wi) = 1$, to nearly 2 in the least viscoelastic 0.3 MDa PEO solution and slightly over 4 in the 4 MDa PEO solution. Such a nonlinear electric field dependence of the particle *FE* in PEO solutions is probably associated with the dependence of $G_D(Wi)$ and $G_{EK}(Wi)$ on the electric field via the shear rate in the definition of Wi in eq 1.

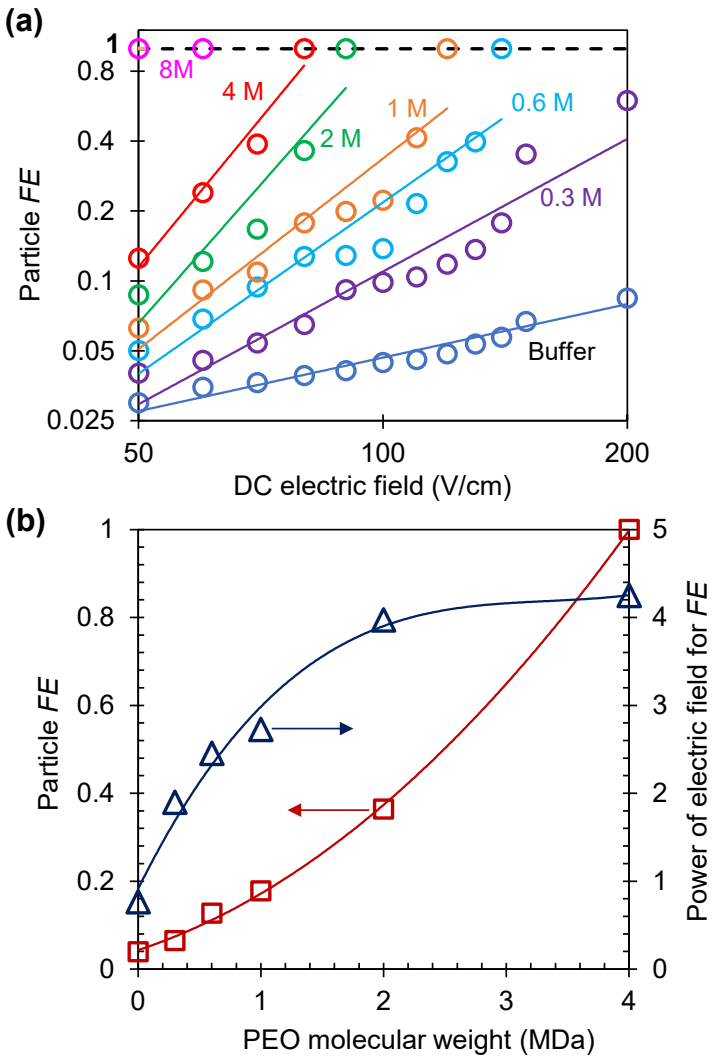

Figure 4. Effect of PEO molecular weight on the iDEP focusing of 10 μm diameter particles in 50 ppm PEO solutions: (a) comparison of the particle focusing effectiveness, *FE*, in the Newtonian buffer and PEO solutions over a range of DC electric fields, where the power trendlines are used to fit the experimental data (symbols); (b) plot of the particle *FE* at 80 V/cm and the power of electric field dependence of *FE* [i.e., the slope of the power trendlines in the log-log space of (a)] vs. the PEO molecular weight, where the lines are used here to guide the eyes only.

Effect of Polymer Concentration

Figure 5 shows the images of 10 μm particles in 2 MDa PEO solutions with concentration varying from 30 to 400 ppm in the constricted microchannel. Analogous to the observations in both Figures

2 and 3, the iDEP focusing of particles in each concentration of PEO solution also gets better with the increase of the imposed DC electric field. It, however, does not exhibit a monotonically increasing trend with the increase of PEO concentration for each electric field case even though the value of Wi increases like that when the PEO molecular weight increases in Figure 3. Specifically, the single-line particle focusing is achieved at 130 V/cm in 30 ppm PEO solution. This required electric field drops to 90 V/cm in 50 ppm PEO (see Figure 2) and then to 80 V/cm in 100 ppm PEO. Also dropped is the electric field for the observed partial trapping of particles, which decreases from around 140 V/cm in 30 ppm PEO to slightly above 100 V/cm in 100 ppm PEO. Such an increasing trend in E-iDEP focusing and trapping may still be explained by the decreasing correction factors, $G_D(Wi)$ and $G_{EK}(Wi)$, in eqs. 4 and 6 because of the increase of Wi. Further increasing the PEO concentration, however, causes the required electric field for single-line particle focusing to rise back to around 120 V/cm in 200 ppm PEO and even higher than 200 V/cm in 400 ppm PEO. This reversed trend is not predicted by eq 4, for which the underlying reason is currently unknown. It might be related to the increasing entanglement of the PEO polymer when the solution gradually approaches the overlapping concentration (see Table 1).

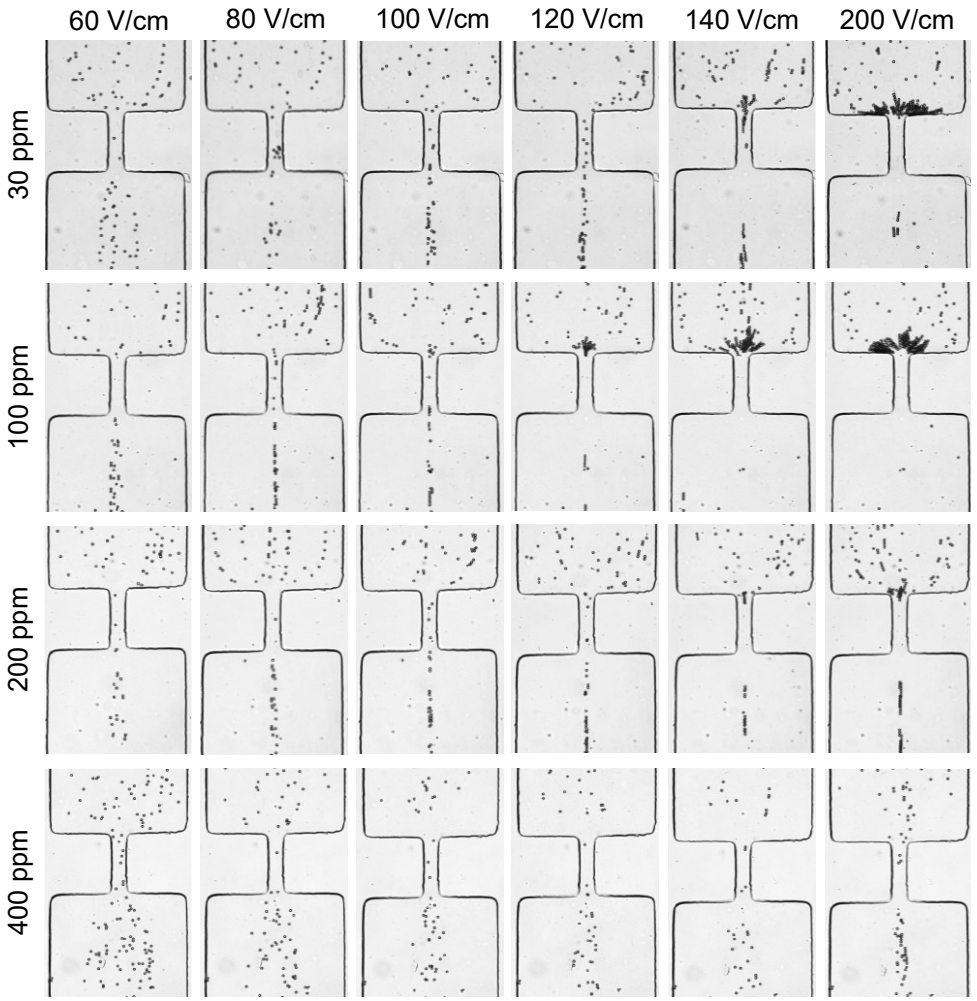

Figure 5. Top-view snapshot images demonstrating the effect of PEO concentration (labeled to the left of each row) on the E-iDEP focusing of 10 μm diameter particles in 2 MDa PEO solutions in the constricted microchannel. The magnitude of the imposed DC electric field is labeled at the top of each column. The particle moving direction is from top to bottom in all images.

Figure 6a shows the experimentally determined particle *FE* vs. DC electric field for 2 MDa PEO solutions with different concentrations. Those values of particle *FE* under a fixed DC electric field of 80 V/cm are also plotted in Figure 6b as a function of the PEO concentration. Analogous to Figure 4a for the effect of PEO molecular weight, the experimental data in each concentration of PEO solution are fitted to a power trendline in Figure 6a. The slope of this trendline in the log-

log space gives the power of electric field dependence of the particle *FE*, which, as viewed from Figure 6b, first increases quickly from roughly 1 in the Newtonian buffer to nearly 5 in 100 ppm PEO solution and then drops to around 2.5 in 200 ppm PEO solution. Finally, the particle *FE* in 400 ppm PEO recovers the almost linear dependence on electric field with the power back to approximately unity. Such a non-monotonic trend in the power of electric field dependence on the PEO concentration is seen in Figure 6b to correlate well with the particle *FE* at 80 V/cm. We also note that the decreasing E-iDEP focusing effect in higher-than-100 ppm PEO solutions shows consistency with our recent work, where the particle focusing in 1000 ppm PEO solution was found to actually become slightly weaker than that in the Newtonian buffer.[51] These observations together may imply the growing role of polymer entanglement in semidilute to concentrated PEO solutions, which has been found in recent papers to have a strong impact on the cross-stream particle migration in a combined pressure and electric field-driven flow.[72]

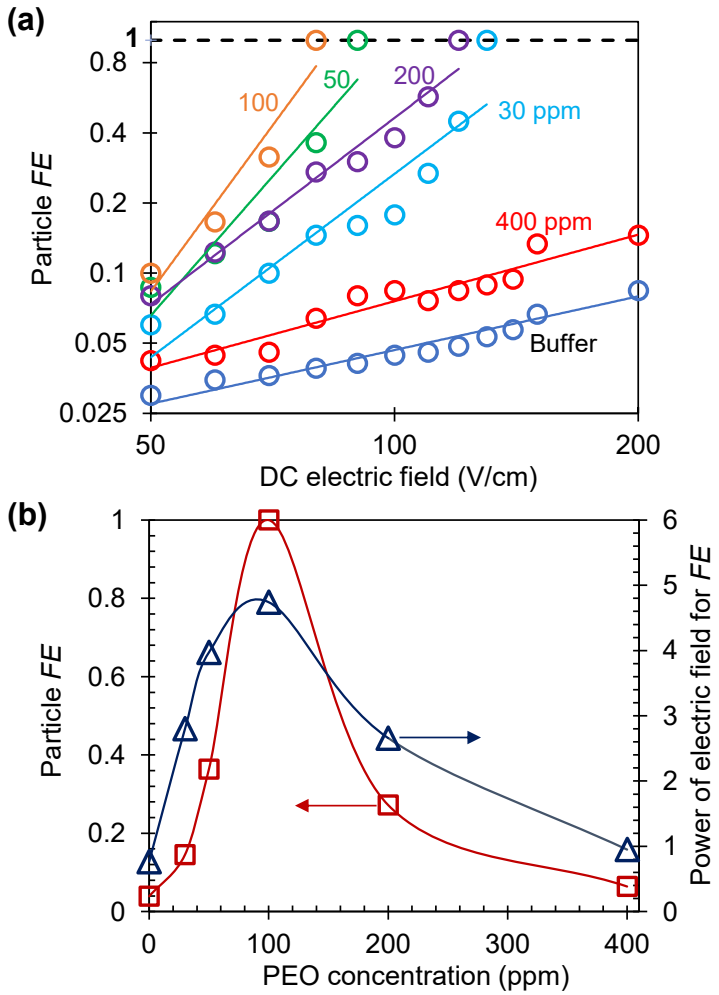

Figure 6. Effect of PEO concentration on the iDEP focusing of 10 μm diameter particles in 2 MDa PEO solutions: (a) comparison of the particle focusing effectiveness, *FE*, in the Newtonian buffer and PEO solutions over a range of DC electric fields, where the power trendlines are used to fit the experimental data (symbols); (b) plot of the particle *FE* at 80 V/cm and the power of electric field dependence of *FE* [i.e., the slope of the power trendlines in the log-log space of (a)] vs. the PEO concentration, where the lines are used here to guide the eyes only.

Effect of Particle Size

Figure 7 shows the images of 5 and 15 μm diameter particles in 50 ppm, 2 MDa PEO solutions in the constricted microchannel under different DC electric fields. Compared to 10 μm particles in Figure 2a, 5 μm particles experience an apparently weaker E-iDEP focusing because of the

quadratic dependence of the dielectrophoretic-to-electrokinetic mobility ratio, β in eq 4, on the particle size. They are not able to achieve a single-line focusing until the electric field is increased to around 200 V/cm. In contrast, 15 μm particles should exhibit a stronger E-iDEP focusing and trapping than 10 μm particles due to the same reason as explained above. Indeed, the required electric field for single-line focusing of 15 μm particles is slightly greater than 70 V/cm, as compared to 90 V/cm for 10 μm particles in Figure 2a. The partial trapping of 15 μm particles also occurs earlier at a smaller electric field than that of 10 μm particles.

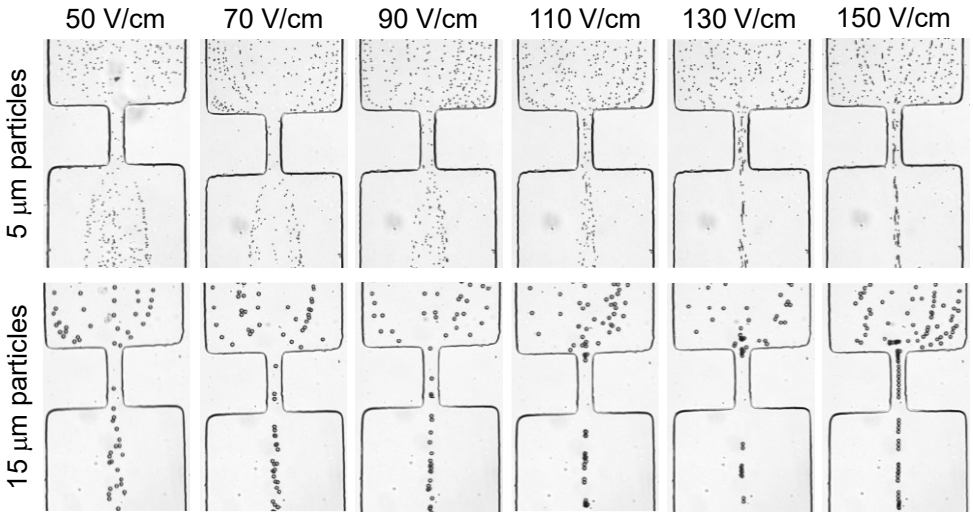

Figure 7. Top-view snapshot images demonstrating the effect of particle size (labeled to the left of each row) on the E-iDEP focusing of particles in 50 ppm, 2 MDa PEO solutions in the constricted microchannel. The magnitude of the imposed DC electric field is labeled at the top of each column. The particle moving direction is from top to bottom in all images.

Figure 8a displays the obtained particle *FE* against electric field, where the experimental data for each particle size are again fitted with a power trendline. The values of *FE* at each electric field show an increasing trend with the particle diameter as demonstrated in Figure 8b for particle *FE*

at 80 V/cm. Figure 8b also shows the power of electric field dependence of the obtained particle *FE* in Figure 8a, which increases from around 2 for 5 μm particles to around 4 for 10 μm particles and slighter higher than 4 for 15 μm particles. This varying power of electric field dependence indicates that one or both of the correction factors, $G_D(Wi)$ and $G_{EK}(Wi)$, in eq 4 may be a function of particle size. It is noted that recent theoretical studies have predicted the particle size-dependent electrophoretic velocity and hence $G_{EK}(Wi)$ in viscoelastic fluids[64,65] because the polymer elasticity-induced extensional stress around a particle varies with its size. We will conduct experiments in future work to investigate how the fluid rheological effects may affect the electrophoretic (or alternatively electrokinetic) velocity of particles with different sizes or charges in straight rectangular microchannels.

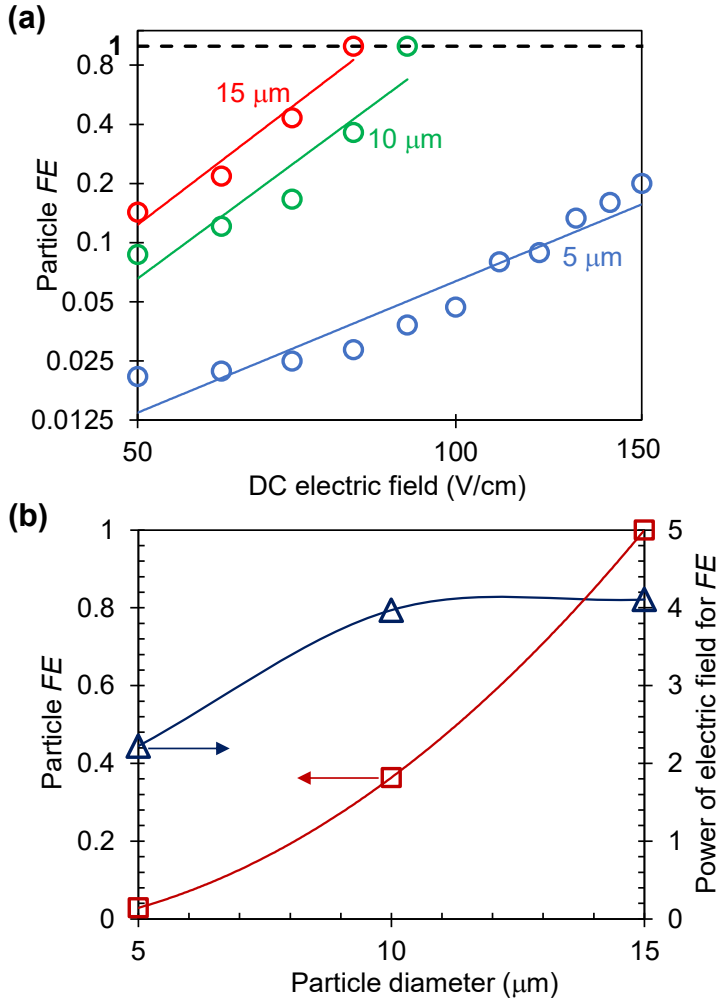

Figure 8. Effect of particle size on the E-iDEP focusing of particles in 50 ppm, 2 MDa PEO solutions: (a) comparison of the particle focusing effectiveness, *FE*, over a range of DC electric fields, where the power trendlines are used to fit the experimental data (symbols); (b) plot of the particle *FE* at 80 V/cm and the power of electric field dependence of *FE* [i.e., the slope of the power trendlines in the log-log space of (a)] vs. the particle diameter, where the lines are used here to guide the eyes only.

CONCLUSIONS

We have experimentally demonstrated the addition of a small amount of PEO polymer into a Newtonian buffer solution can substantially reduce the electric field for sheath-free particle

focusing in a constricted microchannel. In particular, the threshold electric field for single-line focusing of 10 μm particles in 50 ppm, 8 MDa PEO solution is almost one order of magnitude smaller than that in the Newtonian buffer because of E-iDEP. This feature can help maintain the viability of cells in electrokinetic microfluidic devices and hence further broaden the biomedical applications of iDEP. We have also conducted experiments to understand the effects of fluid and particle related parameters on E-iDEP focusing. It is found that the particle *FE* gets enhanced with the increasing PEO molecular weight or particle size. Moreover, their growth trends both flatten out for larger molecular weight and particle diameter, respectively, in terms of the power of electric field dependence of *FE*. Interestingly, the particle *FE* does not follow a similar monotonic trend with the increase of the PEO concentration. The best concentration for particle focusing in 2 MDa PEO solutions is around 100 ppm. We have also developed a theoretical analysis of E-iDEP for particle focusing through the introduction of two fluid elasticity-responsible correction factors. Our analysis is able to explain the impacts of the PEO molecular weight and particle size on the *FE*, but fails for the PEO concentration indicating perhaps the missing of some physics in the theory. Future work is needed for determining the correction factors such that our model may become a useful predictive tool for microfluidic applications employing E-iDEP.

ACKNOWLEDGEMENTS

This work was supported in part by NSF under grant numbers CBET-2100772 and CBET-2127825, and by Clemson University through the Creative Inquiry Program.

REFERENCES

(1) Berlanda, S. F.; Breitfeld, M., Dietsche, C. L., Dittrich, P. S. Recent advances in microfluidic technology for bioanalysis and diagnostics. *Anal. Chem.* **2021**, *93*, 311−331.

(2) Wang, L.; Qi, W.; Liu, Y.; Essien, D.; Zhang, Q.; Lin, J. Recent advances on bioaerosol collection and detection in microfluidic chips. *Anal. Chem.* **2021**, *93*, 9013–9022.

(3) Diaz-Armas, G. G.; Cervantes-Gonzalez, A. P.; Martinez-Duarte, R.; Perez-Gonzale, V. H. Electrically driven microfluidic platforms for exosome manipulation and characterization. *Electrophoresis* **2022**, *43*, 327–339.

(4) Vaghef-Koodehi, A.; Lapizco-Encinas, B. H. Microscale electrokinetic-based analysis of intact cells and viruses. *Electrophoresis* **2022**, *43*, 263–287.

(5) Surappa, S.; Multani, P.; Parlatan, U.; Sinawang,P. D.; Kaifi, J.; Akinac, D.; Demirci, U. Integrated “lab-on-a-chip” microfluidic systems for isolation, enrichment, and analysis of cancer biomarkers. *Lab Chip* **2023**, *23*, 2942-2958.

(6) Xuan, X.; Zhu, J.; Church, C. Particle focusing in microfluidic devices. *Microfluid. Nanofluid.* **2010**, *9*, 1-16.

(7) Yan, S.; Zhang. J.; Yuan. D.; Li, W. Hybrid microfluidics combined with active and passive approaches for continuous cell separation. *Electrophoresis* **2017**, *38*, 238-49.

(8) Gong, Y.; Fan, N.; Yang, X.; Peng, B.; Jiang, H. New advances in microfluidic flow cytometry. *Electrophoresis* **2019**, *40*, 1212-1229.

(9) Song, Y.; Li, D.; Xuan, X. Recent advances in multi-mode microfluidic separation of particles and cells. *Electrophoresis* **2023**, *44*, 910-937.

(10) Guo, W.; Tao, Y.; Mao, K.; Liu, W.; Xue, R.; Ge, Z.; Ren, Y. Portable general microfluidic device with complex electric field regulation functions for electrokinetic experiments. *Lab Chip* **2023**, *23*, 157-167.

(11) Devendran, C.; Choi, K.; Han, J.; Ai, Y.; Neild, A.; Collins, D. J. Diffraction-based acoustic manipulation in microchannels enables continuous particle and bacteria focusing. *Lab Chip* **2020**, *20*, 2674-2688.

(12) Zhang, P.; Bachman, H.; Ozcelik, A.; Huang, T. J. Acoustic microfluidics. *Annu. Rev. Anal. Chem.* **2020**, *13*, 17-43.

(13) Qi, M.; Dang, A.; Yang, X.; Wang, J.; Zhang, H.; Liang, W. Surface acoustic wave manipulation of bioparticles. *Soft Matter* **2023**, *19*, 4166-4187.

(14) Xuan, X. Recent advances in direct current electrokinetic manipulation of particles for microfluidic applications. *Electrophoresis* **2019**, *40*, 2484-2513.

(15) Lapizco-Encinas, B. H. On the recent developments of insulator-based dielectrophoresis: A review. *Electrophoresis* **2019**, *40*, 358-375.

(16) Zhang, K.; Ren, Y.; Hou, L.; Jiang, T; Jiang, H. Flexible particle focusing and switching in continuous flow via controllable thermal buoyancy convection. *Anal. Chem.* **2020**, *92*, 3, 2778–2786.

(17) Xuan, X. Recent advances in continuous-flow particle manipulations using magnetic fluids.

Micromachines **2019**, *10*, 744.

(18) Cao, Q.; Fan, Q.; Chen, Q.; Liu, C.; Han, X.; Li, L. Recent advances in manipulation of micro-and nano-objects with magnetic fields at small scales. *Mater. Horizons* **2020**, *7*, 638-666.

(19) Chong, W. H.; Leong, S. S.; Lim, J. K. Design and operation of magnetophoretic systems at microscale: Device and particle approaches. *Electrophoresis* **2021**, *42*, 2303-2328.

(20) Martel, J. M.; Toner, M. Inertial focusing in microfluidics. *Annu. Rev. Biomed. Eng.* **2014**, *16*, 371–396.

(21) Zhang, J.; Yan, S.; Yuan, D.; Alici, G.; Nguyen, N. T.; Warkiani, M. E.; Li, W. Fundamentals and applications of inertial microfluidics: a review. *Lab Chip* **2016**, *16*, 10–34.

(22) Xiang, N.; Ni, Z. Inertial microfluidics: current status, challenges, and future opportunities. *Lab Chip* **2022**, *22*, 4792-804.

(23) Chen, N.; Zhou, Z.; Zhu, Z.; Jiang, D.; Xiang, N. Controllable size-independent three-dimensional inertial focusing in high-aspect-ratio asymmetric serpentine microchannels. *Anal. Chem.* **2022**, *94*, 15639–15647.

(24) Lu, X.; Liu, C.; Hu, G.; Xuan, X. Particle manipulations in non-Newtonian microfluidics: A review. *J. Colloid Interf. Sci.* **2017**, *500*, 182-201.

(25) Yuan, D.; Zhao, Q.; Yan, S.; Tang, S.; Alici, G.; Zhang, J.; Li, W. Recent progress of particle migration in viscoelastic fluids. *Lab Chip* **2018**, *18*, 551-567.

(26) Zhou, J.; Papautsky, I. Viscoelastic microfluidics: Progress and challenges. *Microsys. Nanoeng.* **2020**, 6, 113.

(27) Bai, J.; Zhang, X.; Wei, X.; Wang, Y.; Du, C.; Wang, Z.; Chen, L.; Wang, J. Dean-flow-coupled elasto-inertial focusing accelerates exosome purification to facilitate single vesicle profiling. *Anal. Chem.* **2023**, *95*, 2523–2531.

(28) Regtmeier, J.; Eichhorn, R.; Viefhues, M.; Bogunovic, L.; Anselmetti, D. Electrodeless dielectrophoresis for bioanalysis: Theory, devices and applications. *Electrophoresis* **2011**, *32*, 2253-2273.

(29) Lapizco-Encinas, B. H. Microscale electrokinetic assessments of proteins employing insulating structures. *Curr. Opinion Chem. Eng.* **2020**, *29*, 9-16.

(30) Perez-Gonzalez, V. H. Particle trapping in electrically driven insulator-based microfluidics: Dielectrophoresis and induced-charge electrokinetics. *Electrophoresis* **2021**, *42*, 2445–2464.

(31) Chou, C. F., Zenhausern, F. Electrodeless dielectrophoresis for micro total analysis systems. *IEEE Eng. Med. Biology Mag.* **2003**, *22*, 62-67.

(32) Cummings, E. B. Streaming dielectrophoresis for continuous-flow microfluidic devices. *IEEE Eng. Med. Biology Mag.* **2003**, *22*, 75-84.

(33) Srivastava, S. K.; Gencoglu, A.; Minerick, A. R. DC Insulator dielectrophoretic applications in microdevice technology: A review. *Anal. Bioanal. Chem.* **2010**, *399*, 301-321.

(34) Benhal, P.; Quashie, D.; Kim, Y.; Ali, J. Insulator based dielectrophoresis: Micro, nano, and molecular scale biological applications. *Sensors* **2020**, *20*, 5095. doi:10.3390/s20185095

(35) Lapizco-Encinas, B. H. The latest advances on nonlinear insulator-based electrokinetic microsystems under direct current and low-frequency alternating current fields: a review. *Anal. Bioanalytical Chem.* **2022**, *414*, 885–905.

(36) Zhu, J.; Xuan, X. Dielectrophoretic focusing of particles in a microchannel constriction using DC-biased AC electric fields. *Electrophoresis* **2009**, *30*, 2668-2675.

(37) Xuan, X.; Raghibizadeh, S.; Li, D. Wall effects on electrophoretic motion of spherical polystyrene particles in a rectangular poly(dimethylsiloxane) microchannel. *J. Colloid Interface Sci.* **2006**, *296*, 743–748.

(38) Xuan, X. Review of nonlinear electrokinetic flows in insulator-based dielectrophoresis: from induced charge to Joule heating effects. *Electrophoresis* **2022**, *43*, 167-189.

(39) Voldman, J. Electrical forces for microscale cell manipulation. *Annu. Rev. Biomed. Eng.* **2006**, *8*, 425–454.

(40) Hawkins, B. G.; Smith, A. E.; Syed, Y. A.; Kirby, B. J. Continuous-flow particle separation by 3D Insulative dielectrophoresis using coherently shaped, dc-biased, ac electric fields. *Anal. Chem.* **2007**, *79*, 7291–7300.

(41) Braff, W. A.; Pignier, A.; Buie, C. R. High sensitivity three-dimensional insulator-based dielectrophoresis. *Lab Chip* **2012**, *12*, 1327-1331.

(42) Lu, S. Y.; Malekanfard, A.; Beladi-Behbahani, S.; Zu, W.; Kale, A.; Tzeng, T. R.; Wang, Y.; Xuan, X. Passive dielectrophoretic focusing of particles and cells in ratchet microchannels. *Micromachines* **2020**, *11*, 451.

(43) Cummings, E. B.; Singh, A. K. Dielectrophoresis in microchips containing Arrays of Insulating Posts: Theoretical and Experimental Results. *Anal. Chem.* **2003**, *75*, 4724–4731.

(44) Malekanfard, A.; Beladi-Behbahani, S.; Tzeng, T. R.; Zhao, H.; Xuan, X. AC insulator-based dielectrophoretic focusing of particles and cells in an "infinite" microchannel. *Anal. Chem.* **2021**, *93*, 5947-5953.

(45) D'Avino, G.; Greco, F.; Maffettone, P. L. Particle migration due to viscoelasticity of the suspending liquid and its relevance in microfluidic devices. *Annu. Rev. Fluid. Mech.* **2017**, *49*, 341-360.

(46) Liu, C.; Hu, G. High-throughput particle manipulation based on hydrodynamic effects in microchannels. *Micromachines* **2017**, *8*, 73.

(47) Tian, F.; Feng, Q.; Chen, Q.; Liu, C.; Li, T.; Sun, J. Manipulation of bio-micro/nanoparticles in non-Newtonian microflows. *Microfluid Nanofluid* **2019**, *23*, 68.

(48) Stoecklein, D.; Di Carlo, D. Nonlinear microfluidics. *Anal. Chem.* **2019**, *91*, 296-314.

(49) Lu, X.; Patel S.; Zhang, M.; Joo, S. W.; Qian, S.; Ogale, A.; Xuan, X. An unexpected particle oscillation for electrophoresis in viscoelastic fluids through a microchannel constriction. *Biomicrofluidics* **2014**, *8*, 021802.

(50) Lu, X.; DuBose, J.; Joo, S. W.; Qian, S.; Xuan, X. Viscoelastic effects on electrokinetic particle focusing in a constricted microchannel. *Biomicrofluidics* **2015**, *9*, 014108.

(51) Bentor, J.; Malekanfard, A.; Raihan, M. K.; Wu, S.; Pan, X.; Song, Y.; Xuan, X. Insulator-based dielectrophoretic focusing and trapping of particles in non-Newtonian fluids. *Electrophoresis* 2021, **42**, 2154-2161.

(52) Ko, C. H.; Li, D.; Malekanfard, A.; Wang, Y.; Fu, L.; Xuan, X. Electroosmotic flow of non-Newtonian fluids in a constriction microchannel. *Electrophoresis* **2019**, *40*, 1387-1394.

(53) Ermolina, I.; Morgan, H. The electrokinetic properties of latex particles. *J. Colloid Interface. Sci.* **2005**, *285*, 419–428.

(54) Graessley, W. W. Polymer chain dimensions and the dependence of viscoelastic properties on concentration, molecular weight and solvent power. *Polymer* **1980**, *21*, 258−262.

(55) Wu, S.; Raihan, M. K.; Song, L.; Shao, X.; Bostwick, J. B.; Yu, L.; Pan, X.; Xuan, X. Polymer effects on viscoelastic fluid flows in a planar constriction microchannel. *J Non-Newton. Fluid Mech.* **2021**, *290*, 104508.

(56) Rodd, L. E.; Cooper-White, J. J.; Boger, D. V.; McKinley, G. H. Role of the elasticity number in the entry flow of dilute polymer solutions in micro-fabricated contraction geometries. *J. Non-Newtonian Fluid Mech.* **2007**, *143*, 170−191.

(57) Tirtaatmadja, V.; Mckinley, G. H.; Cooper-White, J. J. Drop formation and breakup of low viscosity elastic fluids: Effects of molecular weight and concentration. *Phys. Fluids* **2006**, *18*, 043101.

(58) Rubinstein, M.; Colby, R. H. *Polymer Physics*; Oxford University Press Inc.: Oxford, U.K., 2003.

(59) Rodd, L. E.; Scott, T. P.; Boger, D. V.; Cooper-White, J. J.; McKinley, G. H. The inertio-elastic planar entry flow of low-viscosity elastic fluids in micro-fabricated geometries. *J. Non-Newtonian Fluid Mech.* **2005**, *129*, 1−22.

(60) Sridharan, S.; Zhu, J.; Hu, G.; Xuan, X. Joule heating effects on electroosmotic flow in insulator-based dielectrophoresis. *Electrophoresis* **2011**, *32*, 2274-2281.

(61) Acharya, A.; Mashelkar, R. A.; Ulbrecht, J. Flow of inelastic and viscoelastic fluids past a sphere. *Rheol. Acta* **1976**, *15*, 454–470.

(62) Chhabra, R. P.; Uhlherr, P. H. T.; Boger, D. V. The influence of fluid elasticity on the drag coefficient for creeping flow around a sphere. *J. Non-Newton. Fluid Mech.* **1980**, *6*, 187–199.

(63) Sigli, D.; Coutanceau, M. Effect of finite boundaries on the slow laminar isothermal flow of a viscoelastic fluid around a spherical obstacle. *J. Non-Newton. Fluid Mech.* **1977**, *2*, 1–21.

(64) Khair, A. S.; Posluszny, D. E.; Walker, L. M. Coupling electrokinetics and rheology: Electrophoresis in non-Newtonian fluids. *Phys. Rev. E* **2012**, *85*, 016320.

(65) Li, G.; Koch, D. L. Electrophoresis in dilute polymer solutions. *J. Fluid Mech.* **2020**, *884*, A9.

(66) Zhao, C.; Yang, C. Electrokinetics of non-Newtonian fluids: a review. *Adv. Colloid. Interface Sci.* **2013**, *201–202*, 94–108.

(67) Cardenas-Benitez, B.; Jind, B.; Gallo-Villanueva, R. C.; Martinez-Chapa, S. O.; Lapizco-Encinas, B. H.; Pérez-González, V. H. Direct current electrokinetic particle trapping in insulator-based microfluidics: Theory and experiments. *Anal. Chem.* **2020**, *92*, 12871−12879.

(68) Bentor, J.; Dort, H.; Chitrao, R.; Zhang, Y.; Xuan, X. Nonlinear electrophoresis of dielectric particles in Newtonian fluids. *Electrophoresis* **2023**, ***44***, 938-946.

(69) Malekanfard, A.; Liu, Z.; Zhao, H.; Song, Y.; Xuan, X. Interplay of induced charge electroosmosis and electrothermal flow in insulator-based dielectrophoresis. *Phys. Rev. Fluids* **2021**, *6*, 093702.

(70) Ruz-Cuen, R.; de los Santos-Ramírez, J. M.; Cardenas-Benitez, B.; Ramírez-Murillo, C. J.; Miller, A.; Hakim, K.; Lapizco-Encinas, B. H.; Perez-Gonzalez, V. H. Amplification factor in DC insulator-based electrokinetic devices: a theoretical, numerical, and experimental approach to operation voltage reduction for particle trapping. *Lab Chip* **2021**, *21*, 4596-4607.

(71) Khair, A. S. Nonlinear electrophoresis of colloidal particles. *Current Opinion Colloid Interface Sci.* **2022**, *59*, 101587.

(72) Serhatlioglu, M.; Isiksacan, Z.; Ozkan, M.; Tuncel, D.; Elbuken, C. Electro-viscoelastic migration under simultaneously applied microfluidic pressure-driven flow and electric field. *Anal. Chem.* **2020**, *92*, 6932–6940.

FOR TABLE OF CONTENTS ONLY